

Synthesis and Comparative Characterization of Electroless Ni–P, Ni–P-nano-Al₂O₃ and Duplex Ni–P/Ni–P-nano-Al₂O₃ Coatings on Aerospace-Graded AA2024 alloy



Rajsekhar Chakrabarti, Souvik Brahma Hota, and Pradipta Basu Mandal

Abstract The essence of electroless coatings is realized by the scientists since last decade, which makes them a vital player in material coating industry. Incorporation of a second phase micro or nanoelement into the Ni–P matrix widens the area of applications for these types of coatings. Researchers are showing their interest to develop more innovative electroless coatings where they are deploying different types of second phase material to enhance their physical, mechanical and chemical properties. Duplex coatings have shown promising capabilities by providing excess hardness, wear and corrosion resistance, which can be attributed to the resultant effect of two consecutive layers of coating. In our research, three different types of electroless nickel phosphorous (EN) coatings were applied on the aerospace-graded AA2024 alloy substrate. The first type was plain Ni–P coating, the second one was a composite coating where nanoalumina was incorporated into the electroless Ni–P matrix, and the third coating was a duplex coating with the inner layer having Ni–P and the outer layer consisting of a Ni–P layer incorporated with nanoalumina particles. Characterization of the deposits by scanning electron microscopy (SEM) along with energy dispersive X-ray spectroscopy (EDS) confirms the production of flawless, adherent coatings onto the substrate. Maintaining the surface roughness at an acceptable level, a great increase in nanohardness was observed that was further enhanced by incorporation of nano-Al₂O₃ particles and provision of one additional external layer in duplex coating. Excellent wear resistance was also evaluated by the nanoscratch test. On the basis of results obtained, this study suggested the superiority of the electroless duplex coating onto AA2024 substrates especially used in aerospace and defence industries.

Keywords Duplex coatings · Nanohardness · Nanoscratch test · Aerospace and defence industries

R. Chakrabarti · P. B. Mandal

Department of Mechanical Engineering, Techno India University, EM-4, Sector V, Salt Lake City, Kolkata, West Bengal 700091, India

S. B. Hota (✉)

Faculty, Department of Mechanical Engineering, Techno India University, EM-4, Sector V, Salt Lake City, Kolkata, West Bengal 700091, India

e-mail: souvik.h@technoindiaeducation.com

1 Introduction

Over the years, the lifespan of manufactured goods over the globe has played a great role in its sales. The fact that a product is indestructible could eventually be the new trend. Looking into the possibilities of a substance being damaged over a period of time can vastly depend on a few factors such as corrosion, lack of strength and thermal resistance. Eventually, finding a solid body with all of the qualities was proved to be hypothetical, and creation of solid alloys to work as a material replacement was expensive, and hence, coating of surfaces with alloys became a solution.

Substances with a great anticorrosive nature were vastly known by those of Ni and its alloys were known to do the job. With the property to be able to be coated around any surface irrespective of its texture and materials, Ni alloys were even more accepted. However, it is not as well reputed with magnesium, being very highly electrochemically active. Ni could only prove a coating, which could fail in case of physical erosion, and the results would be catastrophic.

In electroless duplex coating, two different layers are superimposed to yield a resultant coating, which exhibits drastic increment in hardness, wear resistance and frictional property due to the combined effect of both contributory layers. Introducing the second phase nanoalumina (Al_2O_3) into the Ni–P matrix of outer layer of the duplex coating will enhance further improvement of the coating qualities. Studies had been made and combinations were revealed for different surfaces, such as Duplex Ni–P/Ni–W–P coatings on AZ31B magnesium alloy [1], duplex electroless NiP/NiB coatings, with Nickel–phosphorous as the internal layer on 2024 aluminium alloys [2] and mild steel [3], Duplex Ni–P–ZrO₂/Ni–P coating on stainless steel [4] and of Duplex Ni–P–TiO₂/Ni–P nanocomposite coating onto brass substrates [5] etc. to name a few.

In this study, basically, three types of electroless coatings have been produced by using hypophosphite reduced bath, and nanosized alumina (Al_2O_3) is used as the second phase dispersed particle due to its high elastic modulus, great wear resistance and high stability at elevated temperature. An optimum concentration of alumina (Al_2O_3) has to be maintained in the electroless coating bath to achieve the desired level of mechanical and allied properties [6]. The reasons behind choosing AA2024 alloy as the substrate for our experiment are an enormous amount of strength and fatigue resistance, which has widened its application in aircraft structural parts, especially wing and fuselage structures under tension. In spite of having those lucrative properties AA2024 shows poor resistance to corrosion, which drives us to develop these coatings over it. To achieve excellent corrosion resistance, high phosphorus Ni–P coating was prepared as the inner layer, while low phosphorus outer layer that is sol-enhanced Ni–P– Al_2O_3 coating was deposited to strengthen the mechanical property. Varying percentage of phosphorus in the inner and outer layers was simply achieved by changing the phosphoric acid (H_3PO_4) content in the bath. Morphology, composition, mechanical properties of all the coatings were systematically investigated in this paper.

Table 1 Chemical composition of AA2024 alloy substrate

Chemical composition [wt.%]						
Cu	Mn	Mg	Si	Fe	Zn	Ti
4.1	0.6	1.4	0.5	0.5	0.25	0.15

2 Experimental Details

2.1 Surface Preparation

The AA2024 alloy sheet of 2 mm thickness that is basically used for flap material is procured from Air India maintenance section and cut into 20×20 mm of pieces, which is suitable for our electroless coating arrangement. The chemical composition of the substrate is presented in Table 1. One corner side of the square-shaped sample was drilled to make small hole for hanging the sample during coating process. The surface of the substrate was ground and polished with 320, 800, 1200, 2000 grit SiC (emery) paper to maintain the roughness of the surface nearly $0.2 \mu\text{m}$ [7].

Final polishing with diamond abrasion paper is carried out after all consecutive grinding and polishing were performed. This made a smoother substrate surface with negligible amount of unevenness needed for the coating.

2.2 Pretreatment and Activation

Pretreatment process includes keeping the sample in soap water at 40°C for 5 min, which is followed by acetone cleaning for removing dust and dirt from the surface. After a thorough cleaning, the sample is subjected to acid pickling for getting oil and grease-free surface with 10% HCl. Finally, samples are required to be activated before putting into the electroless bath. Generally, there are some recommendations to use Ni striking [1] or PdCl_2 solution [8] activation technique in various researches; here we use a combination of PdCl_2 and SnCl_2 solution with proper proportion of the constituents to make a activator solution for our experiment. Although we tried with our very own two-step acid activation technique to minimize the cost but results are not satisfying as it leads to corrosion of AA2024 substrate. After completion of the combination of PdCl_2 and SnCl_2 solution activation, samples are readily dipped into the electroless solution, which already attains an initial temperature of 80°C and pH of 5.5.

2.3 Bath Preparation

Electroless bath for each type of coating comprises some basic constituents like a source of nickel ion, a reducing agent, a stabilizer, a complexing agent and the buffer, which are more or less same for all the three types of electroless coating solution for our experiment. A surfactant is the additional chemical needed for increasing the wettability of the second phase nanoalumina (Al_2O_3) particle to have a better inclusion in Ni–P matrix to develop good nanocomposite and duplex nanocomposite coating. The details of bath compositions of electroless Ni–P, Ni–P-nano- Al_2O_3 composite and duplex Ni–P/Ni–P-nano- Al_2O_3 composite coatings are shown in Table 2.

The bath composition for duplex coating shown in Table 2 is for the second bath, which is used to get outer coating of Ni–P-nano- Al_2O_3 . Inner Ni–P coating will be developed by the bath composition used for plain Ni–P coating as shown in the Table 2. All the constituents of the bath need to mix with required amount of distilled water solution and stirred well in a Borosil beaker with the help of a magnetic stirrer (Tarsons Spinot). A mercury in-glass thermometer (Erose, Maximum range: 360 °C) is placed inside the bath to measure temperature and a universal pH indicator (Merck) is used to get the pH of the bath.

Table 2 Chemical composition of the bath

Constituents	Ni–P	Ni–P-nano- Al_2O_3	Duplex-P/Ni–P-nano- Al_2O_3
Metal ions	Nickel Sulphate 35 g/l	Nickel Sulphate 35 g/l	Nickel Sulphate 35 g/l
Reducing agents	Sodium Hypophosphite 15 g/l	Sodium Hypophosphite 15 g/l	Sodium Hypophosphite 15 g/l
Complexant	Sodium Succinate 12 g/l	Sodium Succinate 12 g/l Sodium Acetate 5 g/l	Sodium Succinate 10 g/l Sodium Acetate 5 g/l Sodium Citrate 5 g/l
Stabilizers	–	Lead Acetate 1 mg/l	Lead Acetate 2 mg/l
Surfactant	–	Sodium Dodecyl Sulphate 0.2 g/l	Sodium Dodecyl Sulphate 0.2–0.4 g/l
Second phase particle	–	Nano- Al_2O_3 (APS:20-30 nm) 5 g/l	Nano- Al_2O_3 (APS:20-30 nm) 5 g/l
	–	H_3PO_4	H_3PO_4
Temperature	80–90 °C	85–90 °C	82–90 °C
pH	5–6	4.5–5.5	4.5–5.5
Time	2 h	2.5 h	3 h

2.4 Nanoalumina Sol Preparation

Nanoalumina (Al_2O_3) powder is collected from Sisco Research Laboratories (SRL) with average particle size of 20–30 nm. Sol of 5 g/l nano- Al_2O_3 powder is prepared by mixing it with 15 ml of distilled water by ultrasonic agitator (LABMAN) for 15 min. For the electroless Ni–P-nano- Al_2O_3 composite coating, the sol is to be added after the first hour of coating. In case of duplex coating, this has to be added to the second solution for the outer layer of the coating only after 30 min of coating. The dispersion of second phase nanoalumina particle is maintained by proper stirring done by a magnetic stirrer cum heater (TarsonsSpinot) used for our experiment.

2.5 Sample Characterization

The surface morphology of electroless Ni–P, Ni–P-nano- Al_2O_3 composite and duplex Ni–P/Ni–P-nano- Al_2O_3 composite coating is assessed by Scanning Electron Microscope (HITACHI S-3400 N). HORIBA EMAX Si (Li)-Liquid nitrogen cooling type x-ray detector, which is integrated with the SEM, is used for composition analysis of these coatings. Nanoindentation test is performed to evaluate the individual hardness of the coating and also to justify the purpose of nanoalumina inclusion along with the duplex coating. A CSM NHTX S/N: 55-0019 nanohardness tester (NHT) calibrated on pure silica and aluminium and used for this purpose. A triangular pyramidal diamond indenter (Berkovichtip, B-I 93) with a tip radius of 0.2 μm under a constant load of 10 mN and the pause time was 2 s. The loading rate was 20 mN/min, and unloading rate was also kept at 20 mN/min with a data acquisition rate of 10 Hz. The hardness was calculated using the Oliver-Pharr analysis method [9–11], which could be executed from the software provided by CSEM Instruments. Instrumented elastic moduli (EIT) were estimated from the initial gradient of the unloading curves using the Oliver and Pharr [12] model. Nanoscratch test was performed using CSM NST: 50–133 nanoscratch tester under a normal load of 5 mN with a scratching speed of 1.2 mN/min, and the length of the scratch was ~ 5 mm to measure the wear rate of the coatings. A typical single scratch test has been carried out on the coating with a loading rate of 10 mN/min. The Sphero-conical diamond indenter's (SB-A63) tip radius was 2 μm .

3 Results and Discussions

3.1 Surface Morphology and Composition

SEM micrographs of Ni–P-nano- Al_2O_3 composite coating with concentrations of 5 g/L of alumina (Al_2O_3) are shown in Fig. 1b. In Ni–P-nano- Al_2O_3 coating, second

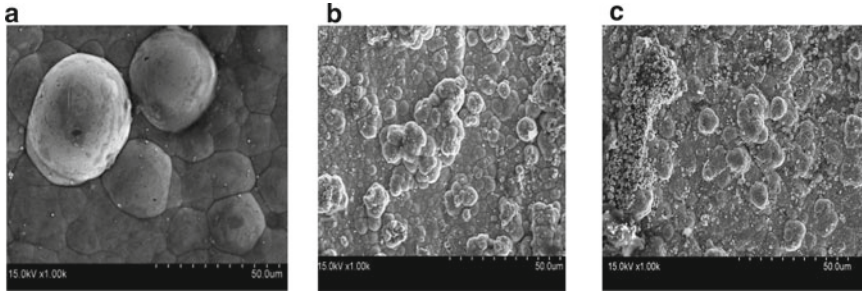


Fig. 1 SEM micrograph of various electroless coatings. **a** Ni-P coating, **b** Ni-P-nano- Al_2O_3 composite coating, **c** Duplex Ni-P-nano- $\text{Al}_2\text{O}_3/\text{Ni-P}$ composite coating

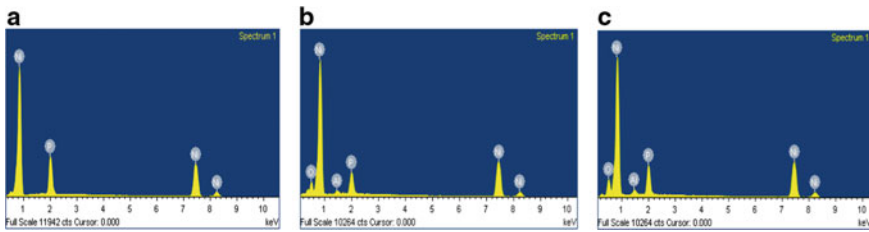


Fig. 2 Composition of various electroless coatings. **a** Ni-P coating, **b** Ni-P-nano- Al_2O_3 composite coating, **c** Duplex Ni-P-nano- $\text{Al}_2\text{O}_3/\text{Ni-P}$ composite coating

phase white nanoalumina particles are successfully co-deposited and uniformly distributed throughout the Ni-P matrix. The alumina particles take their place in Ni-P matrix. The co-deposition of nano- Al_2O_3 particles increases the catalytic active sites and, thus, increases the reduction of nickel ions. The randomly adsorbed nano- Al_2O_3 particles on the surface were covered by nickel due to further reduction reaction, which leads to dim surface of the coating compared to plain Ni-P coating. No superficial surface damage is found, and the coating appears to be dense.

The EDX analyses of coated samples are shown in Fig. 2a–c. The peaks shown in Fig. 2a of nickel and phosphorous are quite specific with respect to the obtained parameters in this experiment. Figure 2b, c shows additional peaks of aluminium and oxygen, which confirms the inclusion of second phase nanoalumina particles in Ni-P matrix for the last two cases where we suppose to prepare electroless Ni-P-nano- Al_2O_3 composite coating and duplex Ni-P-nano- $\text{Al}_2\text{O}_3/\text{Ni-P}$ composite coating.

3.2 Hardness

Figure 3 shows the typical load versus depth of indentation curve of Ni-P, Ni-P-nano- Al_2O_3 composite and duplex Ni-P/Ni-P-nano- Al_2O_3 composite coatings, in

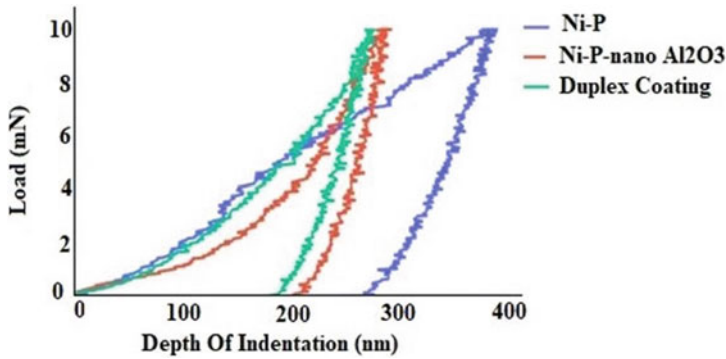


Fig. 3 Load–displacement curves for Ni–P, Ni–P-nano- Al_2O_3 composite and duplex Ni–P/Ni–P-nano- Al_2O_3 composite coatings during nanoindentation test

which residual depth (h_r), maximum depth (h_{\max}) have been shown. Ni–P coating exhibits h_r value of 313.83 nm while the value is 232.99 nm for Ni–P-nano- Al_2O_3 composite coating, and for duplex Ni–P-nano- Al_2O_3 coating, the value is 216.77 nm. Hence, $\sim 25.75\%$ reduction in residual depth of Ni–P-nano- Al_2O_3 composite coating was observed, and for duplex Ni–P-nano- Al_2O_3 /Ni–P composite coating there is a reduction of $\sim 6.96\%$ in residual depth, indicating the increase in hardness of the Ni–P-nano- Al_2O_3 and duplex Ni–P-nano- Al_2O_3 /Ni–P composite coatings. The average hardness value for Ni–P coating was 278.02 Hv. It gets increased to 654.62 Hv in case of Ni–P-nano- Al_2O_3 composite coating. Further increase in hardness is found in case of duplex Ni–P-nano- Al_2O_3 /Ni–P composite coating up to 828.67 Hv. Improvement in hardness nanocomposite coating could be attributed to the incorporation of the hard Al_2O_3 particles in the coating. The duplex Ni–P-nano- Al_2O_3 /Ni–P composite coating achieved higher hardness due to two consecutive factors; (a) development of dual layer and (b) incorporation of nano- Al_2O_3 particles in the outer layer.

3.3 Elastic Modulus

Instrumented elastic modulus (E_{IT}) for electroless Ni–P coating is found to be 60.957 GPa, for Ni–P-nano- Al_2O_3 composite coating the value of instrumented elastic modulus is increased to 145.09 GPa with a drastic improvement of 138%. This shows the inclusion of nano- Al_2O_3 particles in the Ni–P matrix makes the coating capable enough to resist deformation. Duplex Ni–P/Ni–P-nano- Al_2O_3 composite coating shows further improvement in elastic modulus up to 150.94 GPa (4.03% increment). This attributes the fact of additional outer layer of duplex coating gives some percentages of additional resistance to deformation. These increments of elastic modulus establish the fact of increased hardness for nanocomposite and duplex coatings.

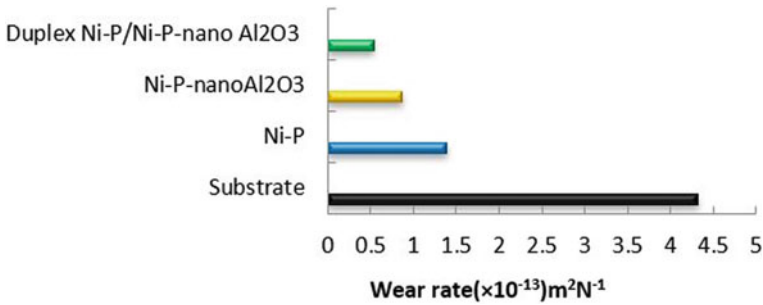


Fig. 4 Wear rate for different coatings and substrate as per nanoscratch test

3.4 Wear Resistance

At a constant load of 5 mN, the wear rate of the scratch of electroless Ni-P coating was found to be $1.39 \times 10^{-13} m^2 N^{-1}$ while the wear rate of the scratch of Ni-P-nano- Al_2O_3 coating was observed to be $0.87 \times 10^{-13} m^2 N^{-1}$, and for duplex Ni-P-nano- Al_2O_3 /Ni-P composite coating, it was much reduced to $0.54 \times 10^{-13} m^2 N^{-1}$. The wear rate for different coatings is shown in Fig. 4. The weight loss during the nanoscratch test for AA2024 substrate is highest under the applied load. Lesser weight loss in case of the coated samples shows their better wear resistance than that of AA2024 substrate. Incorporation of nanosized alumina is observed to increase the wear resistance of the coating in last two cases. Additional improvement in wear resistance for duplex Ni-P-nano- Al_2O_3 /Ni-P composite coating can be attributed to the combined effort of dual layer of this coating.

4 Conclusions

Co-deposition of alumina particles in Ni-P electroless coating changes surface morphology of deposits with alumina in Ni-P-nano- Al_2O_3 composite coating and duplex Ni-P-nano- Al_2O_3 /Ni-P composite coating. Cauliflower-type spherical shapes are formed for Ni-P coating, which are basically having 30–40 μm of diameter. These spheres are nickel and smaller nodular structure represents phosphorous. Nanoalumina (Al_2O_3) when included with Ni-P matrix produces nanocomposite coating, and the whitish and blackish small particles in SEM image are nothing but the included alumina particles in the composite coating. Same particle inclusion also takes place in the outer layer of duplex coating, which is confirmed in composition analysis. Ni-P coating shows 278.02 Hv of hardness value, which increased about 135% in case of Ni-P-nano- Al_2O_3 coating, which is mainly attributed to the inclusion of hard alumina particles into the Ni-P matrix. Along with this particle inclusion effect, it is observed that there is an increment of 26.58% in hardness value (828.67 Hv) in case of the duplex composite coating. This additional hardness increment is

the resultant effect of inner and outer layer of the coating. Wear resistance is also improved for electroless nanoalumina composite and duplex composite coating, and this can be attributed to the improving hardness value. Therefore, it is revealed from the present experiment that duplex Ni-P-nano- Al_2O_3 /Ni-P composite coating is an excellent protective coating for AA2024 alloy. Electrochemical Impedance Spectroscopy (EIS) is a powerful tool to study the corrosion resistance of coatings, which can be used in the further investigation of the corrosion properties of these coatings.

References

1. Selvi VE, Chatterji P, Subramanian S, Balaraju JN (2014) Autocatalytic duplex Ni-P/Ni-W-P coatings on AZ31B magnesium alloy. *Surf Coat Technol* 240:103–109
2. Vitry V, Sens A, Kanta AF, Delaunois F (2012) Wear and corrosion resistance of heat treated and as-plated Duplex NiP/NiB coating on 2024 aluminum alloys. *Surf Coat Technol* 206
3. Sankara Narayanan TSN, Krishnaveni K, Seshadri SK (2003) Electroless Ni-P/Ni-B duplex coatings: preparation and evaluation of microhardness, wear and corrosion resistance. *Mater Chem Phys* 82: 771–779
4. Wang YX, Shu X, Wei SH, Liu CM, Gao W, Shakoor RA et al (2015) Duplex Ni-P-ZrO₂/Ni-P electroless coating on stainless steel. *J Alloy Compd* 630:189–194
5. Zhang W, Cao D, Qiao Y, He Z, Wang Y, Li X, Gao W (2019) Microstructure and properties of duplex Ni-P-TiO₂/Ni-P nanocomposite coatings. *Mater Res* 22(Suppl. 2): e20180748. Epub
6. Alirezaei S, Monirvaghefi SM, Salehi M, Saatchi A (2004) *Surf Coat Technol* 184:170
7. Karthikeyan S, Vijayaraghavan L (2016) Influence of Nano Al_2O_3 particles on the adhesion, hardness and wear resistance of electroless NiP coatings. *Int J Mater Mech Manuf* 4(2):106–110
8. Gadhari P, Sahoo P (2014) Study of tribological properties of electroless Ni-P- Al_2O_3 composite coatings. *IOSR J Mech Civil Eng*: 34–37
9. Carrasco CA, Vergara V, Benavente R, Mingolo N, Ríos JC (2002) The relationship between residual stress and process parameters in TiN coatings on copper alloy substrates. *Mater Charact* 48:81–88
10. Oliver WC, Pharr GM (2004) Measurement of hardness and elastic modulus by instrumented indentation: advances in understanding and refinements to methodology. *J Mater Res* 19(1):3–20
11. Fischer-Cripps AC (2006) Critical review of analysis and interpretation of nanoindentation test data. *Surf Coat Technol* 200(14–15):4153–4165
12. Oliver WC, Pharr GM (1992) Improved technique for determining hardness and elastic modulus using load and displacement sensing indentation experiments. *J Mater Res* 7(6):1564–1580